

Cite this: DOI: 10.1039/c2lc40840f

www.rsc.org/loc

PAPER

Universal logic gates *via* liquid-electronic hybrid divider†

Bingpu Zhou,^a Limu Wang,^a Shunbo Li,^b Xiang Wang,^a Yu Sanna Hui^{ab} and Weijia Wen^{*ab}

Received 24th July 2012, Accepted 2nd October 2012

DOI: 10.1039/c2lc40840f

We demonstrated two-input microdroplet-based universal logic gates using a liquid-electronic hybrid divider. All 16 Boolean logic functions have been realized by manipulating the applied voltages. The novel platform consists of a microfluidic chip with integrated microdroplet detectors and external electronic components. The microdroplet detectors act as the communication media for fluidic and electronic information exchange. The presence or absence of microdroplets at the detector translates into the binary signal 1 or 0. The embedded micro-mechanical pneumatically actuated valve (PAV), fabricated using the well-developed multilayer soft lithography technique, offers biocompatibility, flexibility and accuracy for the on-chip realization of different logic functions. The microfluidic chip can be scaled up to construct large-scale microfluidic logic computation. On the other hand, the microfluidic chip with a specific logic function can be applied to droplet-based chemical reactions for on-demand bio or chemical analysis. Our experimental results have presented an autonomously driven, precision-controlled microfluidic chip for chemical reactions based on the IF logic function.

Introduction

Droplet-based microfluidics has become an increasingly attractive and quickly evolving research field due to its superiorities such as small volume requirement, short reaction time for rapid analysis, parallel throughput and compatibility in automation.^{1–3} During the past decade, substantive technologies have been widely exploited for microdroplet generation, transportation, fusion and splitting.^{4–8} As an emerging research field, the use of microdroplets as individual reactors in microchannels has been proved to be an effective experimental paradigm for diverse, on-chip biological and chemical applications.^{9–13}

Apart from on-chip miniature reactors, logic computation has been envisioned as another promising application in droplet-based microfluidics. The concept and operation of microfluidic logic functions are in analogy to digital electronics. To date, various approaches have been reported for microfluidic logic computing,^{14,15} such as electrochemical reaction,¹⁶ nonlinearity in fluid viscosity,¹⁷ relative flow resistance,¹⁸ fluorescent molecular logic devices¹⁹ and bubbles travelling in microchannels.²⁰ However, the drawbacks of these techniques, for example, adapting different interpretations for input/output signals and demand for functionalized liquids with nonlinear fluid viscosities, lead to a relatively complicated integration or cascading scheme for large-scale application. When it comes to droplet-

based microfluidics, discrete microdroplet dispersal in a continuous phase liquid provides researchers with a convenient platform for distinguishing signals by defining the presence or absence of a droplet as binary signal 1 or 0, respectively. This inherent “digital” characteristic of microdroplets is the foundation for on-chip logic operation using microfluidic approaches. In 2007, L. F. Cheow *et al.*²¹ presented the AND, OR and NOT logic operations based on digital microfluidics. Their design blueprint relies on the change of hydrodynamic resistance inside the flow channel. Logic gates such as OR/AND, NOR/NAND, and XNOR, which were constructed from diverse microfluidic chip architecture, have already been published by M. W. Toepke *et al.*²² In their work, a programmable autonomous timer has been realized. The electrowetting-on-dielectric (EWOD) system was also introduced as another promising approach for on-chip microfluidic logical computation,²³ however, the pre-defined command of droplet trajectory limits its practicality to some extent.

In our previous work, giant electrorheological fluid (GERF) was introduced as the computational medium for droplet-based universal logic operations.²⁴ All 16 Boolean logic functions have been achieved by the manipulation of the voltages at the inputs. However, the relatively high operating voltage (~ 300 V) for the GERF phase transition restricts the portability of the device. Here, we propose a new design for on-chip universal logic operations based on a liquid-electronic hybrid divider. The hybrid platform is composed of a microfluidic chip with integrated micro-detectors embedded in the microchannels, and an external electronic circuit for signal control, triggering and analysis. The fluidic signal representing the presence or absence of a microdroplet can be “read” by the embedded microdetectors and converted to electrical information due to the change in

^aNano Science and Technology Program and KAUST-HKUST Microfluidic Joint Laboratory, The Hong Kong University of Science and Technology, Clear Water Bay, Kowloon, Hong Kong

^bDepartment of Physics, The Hong Kong University of Science and Technology, Clear Water Bay, Kowloon, Hong Kong.
E-mail: phwen@ust.hk; Fax: 852 2358 1652; Tel: 852 2358 7979

† Electronic supplementary information (ESI) available. See DOI: 10.1039/c2lc40840f

localized impedance. Each logic function has a corresponding set of input voltages (voltage range of ± 9.0 V), and a coherent interpretation scheme of inputs/outputs is crucial for large-scale cascading applications. The maturity of the fabrication technology for on-chip universal logic gates also preserves the possibility of achieving programmable and reconfigurable microfluidic devices, which is critical for the future of microfluidic computational systems. Owing to the bio-compatibility, a universal logic gate based on droplet microfluidics can be a promising approach for various biological or chemical applications.

Principle

The schematic in Fig. 1(a) shows the working principle of the universal logic gates based on a liquid-electronic hybrid divider. The hybrid divider is composed of a microfluidic chip (red dashed rectangle), and an external circuit board (blue dashed rectangle) containing controlling and analyzing circuits. The two components are connected by electrodes embedded inside the microfluidic chip. The microfluidic chip comprises two input signal channels with embedded detectors to monitor the change in impedance, an output signal channel and a pneumatically actuated valve (PAV). Conductive droplets, which are carried by the insulating fluid, can be detected by the embedded sensing electrode pair in the microchannel. Depending on the inherent impedance in the sensing circuit, the presence of conductive droplets at the parallel electrode pair can trigger an equivalent ON/OFF signal as depicted in Fig. 1(b). By defining the voltages at the electrode pads (V_{12} and V_{34} in Fig. 1(a), with a built-in resistance $R_A = R_B \approx 10$ M Ω existing in the circuit loop on the board), the presence of conductive droplets or insulating carrier fluid with distinctive impedances can be converted into electrical signals by analysing the voltage difference (ΔV) at nodes A and B using the analyzing circuit. The voltage differences ($\Delta V = |V_A - V_B|$) are compared and sent to the triggering circuit which in turn drives the solenoid valve and the PAV to generate a corresponding fluidic signal at the output. If ΔV is larger than V_g (the built-in threshold voltage in the triggering circuit), then a driving

voltage will be generated from the triggering circuit to open the solenoid valve. An opened valve permits air to fill up the air passage into the on-chip PAV, which serves as the switch to actuate the output signal in the form of no microdroplet release.

Fig. 1(c) illustrates the working principle of the on-chip PAV. The PAV lies in the valve layer which is above the flow channel for the output signal known as the flow layer. In between these two layers, a thin polydimethylsiloxane (PDMS) membrane will deflect downwards if air pressure is applied to the PAV, resulting in the passage below being sealed.²⁵ The air-filled PAV then gives rise to an OFF state at the output. Once the pressure is released, the membrane will resume its original state, producing a corresponding ON state at the output which is represented by the release of a microdroplet into the output flow channel.

From this perspective, if V_g , V_{12} and V_{34} are fixed at a desired value, the behavior of the output signal will only be controlled by different combinations of input fluidic signal A and B defined by the voltage difference between V_A and V_B . Here we adopt the binary concept in electronics and define “1” to indicate a conductive droplet present at the detecting electrode pair and “0” to represent the presence of insulating carrier fluid. Similarly at the output port, “1” indicates that a signal droplet is released (the PAV is non-deflected) into the continuous phase liquid, while “0” indicates the contrary. In such a liquid-electronic hybrid method, fluid communication and logic computation can be realized simultaneously, where input fluidic signals are converted into electric signals for logic control, and the output signal can be achieved in fluidic form. For a specific logic function, different input combinations of A and B, [e.g. (0, 0), (0, 1), (1, 0) and (1, 1)], are converted into output fluidic signals of “1” and “0”. Other logic functions can therefore be achieved by different combinations of V_{12} and V_{34} .

Methods

Design of microfluidic chip

Fig. 2(a) illustrates the 3D configuration of the microfluidic chip used in the liquid-electronic universal logic gate. The chip

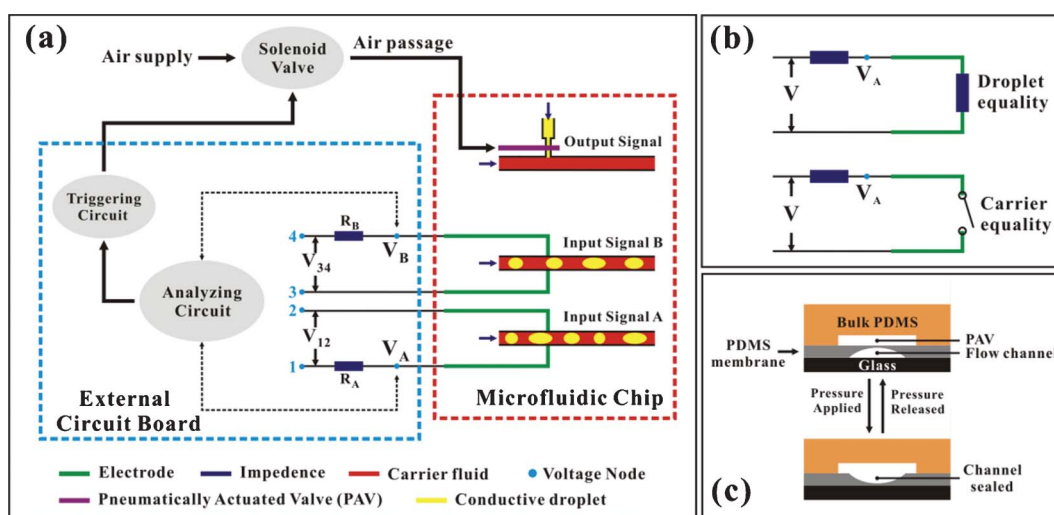


Fig. 1 (a) Working principle of universal logic gates based on liquid-electronic hybrid divider; (b) equivalent circuit for the presence of conductive droplets and insulating carrier fluid at the parallel electrode pair; (c) principle of a PAV controlled switch.

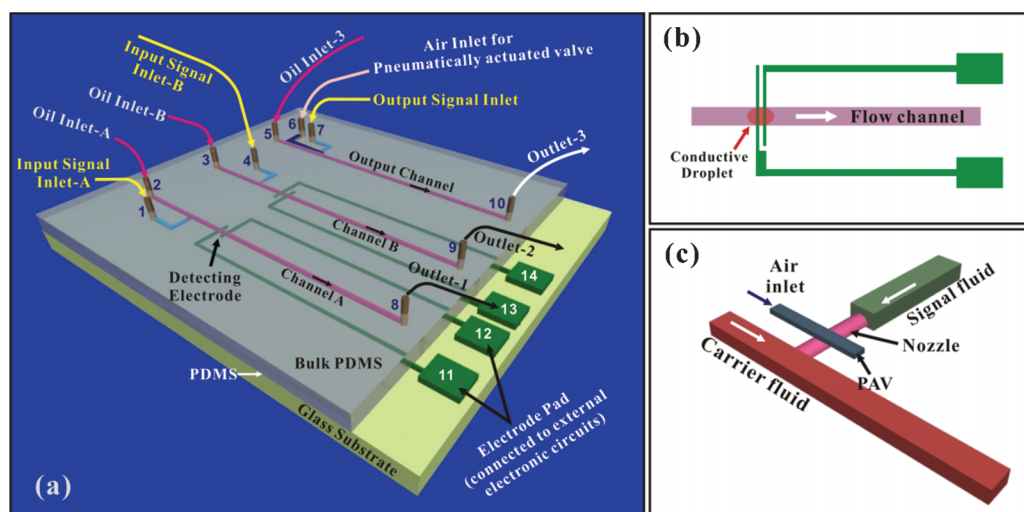


Fig. 2 (a) 3D illustration of the microfluidic chip design; (b) detailed description of the embedded conductive droplet detector; (c) 3D illustration of the on-chip pneumatically actuated valve (PAV).

contains three parallel flow channels, two for input and one for output. For PAV fabrication, a thin PDMS membrane is sandwiched between a thick PDMS slab and the glass substrate, forming a dual-layer architecture as depicted in Fig. 1(c). Two pairs of electrodes are constructed on the glass substrate and embedded in PDMS-based input fluidic channels for detecting conductive droplets, which is the unique on-chip detecting approach used in the universal logic gate design. A diagram showing the droplet detector is depicted in Fig. 2(b). The two on-chip droplet detectors are embedded in the microchannels and each consists of two parallel electrodes which are connected to two external conducting pads. At the moment when the conductive droplet passes above the parallel electrodes, the electric circuit is closed which causes a voltage drop across the resistors, R_A and R_B . The change of impedance is picked up by the external analyzing circuit. Conducting pads numbered from 11 to 14 are used as connections between the on-chip electrodes and the external circuits. The inlets numbered 1, 4 and 7 are for Na_2SO_4 signal injection while the inlets numbered 2, 3 and 5 are for sunflower oil carrier fluid injection. All three flow channels within the microfluidic chip adopt a T-junction design for stable and discrete signal droplet generation based on the mechanism of droplet break-up.^{26,27} The inlet numbered 6 is for air pressure intake, which serves as the driving force for the PAV. The outlets numbered from 8 to 10 are fluid draining ports.

The architecture of the on-chip PAV is outlined in Fig. 2(c). In our design, a narrow nozzle is introduced at a T-junction. A round shape of the nozzle (its detailed fabrication technology will be discussed in the next subsection) achieves better channel sealing, which was discussed in Quake's report.²⁵ The controlling valve placed at the nozzle controls the on-off state of the output fluidic signal.

Microfluidic chip fabrication

The fabrication of the dual-layer microfluidic chips follows standard lithographic protocol. The device consists of three critical components, the pneumatically actuated valve (PAV) layer, the flow channel and the built-in detecting electrodes. The

fabrication process is illustrated in Fig. 3 and explained in detail below.

(a) PAV layer master: negative photoresist SU8-3025 was used to form the PAV layer master. A clean glass substrate was first spin-coated with an 80 μm thick photoresist. Then it was exposed to UV followed by developing. Lastly, a hard-baking process (180 $^\circ\text{C}$ for 1.5 h) was performed to enhance the adhesion.

(b) Flow channel layer master: the materials used in forming the flow channel are photoresists SU8-3025 and PR4903. Two pattern masks were used to form the flow channel layer. One mask formed the main flow channel together with the side flow channel using SU8-3025, and the other formed the narrow nozzle for the main and side channel connection using PR4903.

PR4903 was first spin-coated on the bare glass substrate. After UV-exposure and developing, a baking process (140 $^\circ\text{C}$ for 0.5 h and then 170 $^\circ\text{C}$ for 2 h) was adopted to allow the photoresist to reflow and form a round nozzle. The width and height of the nozzle were $\sim 130 \mu\text{m}$ and $\sim 33 \mu\text{m}$ respectively after the reflow. Then, SU8-3025, with a thickness of about 60 μm , was spin-coated on the patterned glass substrate, followed by alignment, UV exposure and developing processes. A final hard-baking process (180 $^\circ\text{C}$ for 1.5 h) was introduced to improve the material adhesion to the substrate.

(c) Built-in detecting electrodes: positive photoresist PR4620 with a thickness of 10 μm was spin-coated onto a glass substrate and subjected to UV exposure. After developing, a thin metal layer (Ti/Pd: 10/150 nm) was sputtered onto the patterned layer. Titanium was used to enhance the adhesion between the metallic thin film and the substrate. Excess metal film was removed by the lift off process.

(d) Integrated dual-layer microfluidic chip: PDMS gel was prepared by mixing the base with the curing agent in a weight ratio of 10 : 1 and applying it to the PAV layer master. After solidification, the PDMS slab was carefully peeled off from the master, with the valve structure successfully transferred onto the cast. PDMS (15 : 1 weight ratio of base and curing agent) was spin-coated onto the flow channel master to produce a flat membrane of about 100 μm . The PDMS cast with PAV was

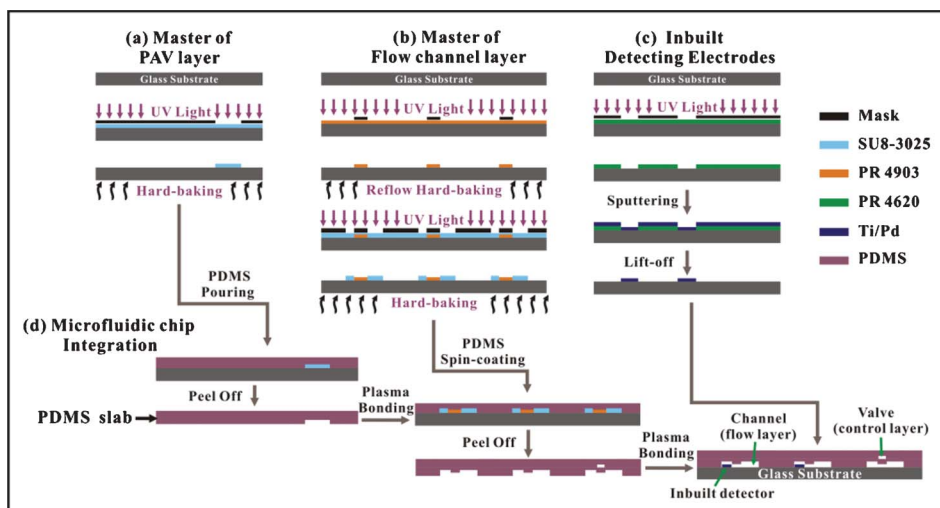


Fig. 3 Fabrication process of the microfluidic chip which consists of the PAV (control layer), built-in detecting electrodes (detector), and microfluidic channels (flow layer).

bonded to the PDMS membrane together with the output nozzle after oxygen plasma surface treatment for 2 min. The PDMS slab with the patterned membrane was stripped from the flow channel master. Oxygen plasma treatment was used for bonding the PDMS slab with the detector pattern on the glass substrate. A final baking process (100 °C, 10 min) concluded the entire chip formation process.

Experimental set-up

The experimental setup for the universal logic gate demonstration is shown in Fig. 4. The setup consists of syringe pumps (KD Scientific, 781200), an optical microscope (SZX2-ILLJ, Olympus Corporation, Japan), an external circuit board and DC dual channel steady voltage supplies (Dual-Tracking DC Power Supply 6303D, Topward Electric Instruments Co., Ltd., Taiwan). Syringe Pumps were used for injecting fluids into the microchannels. The microfluidic chip was placed on a sample holder for observation using the optical microscope. Experimental results were captured by data acquisition card to a computer. The driving voltage for the external circuit board was supplied by the DC voltage supplies. The external circuit board was used for analyzing the fluid signal collected from the

microfluidic chip and converting it into an electric signal which controls the solenoid valve. The solenoid valve (VDW2 50-6G-2-M5) was supplied by SMC Pneumatics (Hong Kong) Ltd.

Materials and reagents

Materials used for the two masters were SU8-3025 negative photoresist (MicroChem Corp., USA), PR4903 (AZ Electronic Materials Hong Kong Limited, Hong Kong) and PR4620 (AZ Electronic Materials Hong Kong Limited, Hong Kong). The microfluidic chips were made of polydimethylsiloxane (PDMS) (Sylgard 184 silicone elastomer kit, Dow Corning Corporation, USA).

Sunflower oil was used as the carrier fluid in the demonstration of the universal logic gate and droplet-based chemical reaction. These experimental details will be discussed in the next section. For the logic function demonstration, sunflower oil was merged with Oil Red O (Sigma-Aldrich Co., USA) for color contrast. Saturated sodium sulfate (Na_2SO_4 , Riedel-de Haën, Sigma-Aldrich Co., USA) solution was to form microdroplets which were dispersed in the continuous phase at the inputs and output. Reagents used in the droplet-based chemical reaction included iron dichloride (saturated FeCl_2 , Sigma-Aldrich Co., USA) and sodium thiocyanate (NaSCN , $\sim 1 \text{ mol L}^{-1}$, Aldrich Chemical Co. Inc., USA).

Results and discussion

Characterization of microfluidic device

Fig. 5(a) shows a photo of the fabricated microfluidic chip. The flow channels were filled with colored sunflower oil for better contrast. All of the inlets and outlets were numbered according to Fig. 2(a). The dimension of the chip is comparable to that of a Hong Kong two dollar coin. The entire chip was about $(2.5 \times 3.5) \text{ cm}^2$. The height and the width of the flow channel were 60 μm and 250 μm respectively. Fig. 5(b) shows the two pairs of built-in electrodes for droplet detection. Each pair of electrodes consists of two parallel palladium lines separated by a 50 μm

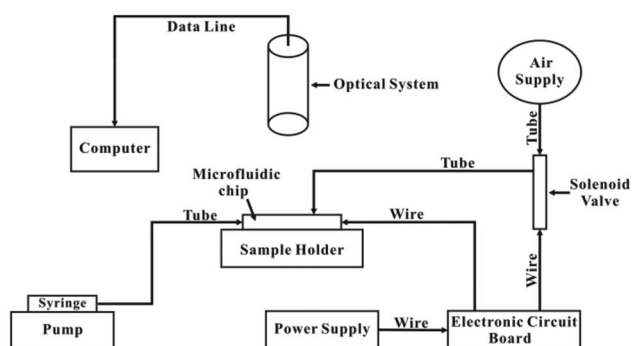


Fig. 4 Schematic showing the experimental setup for the universal logic gate demonstration.

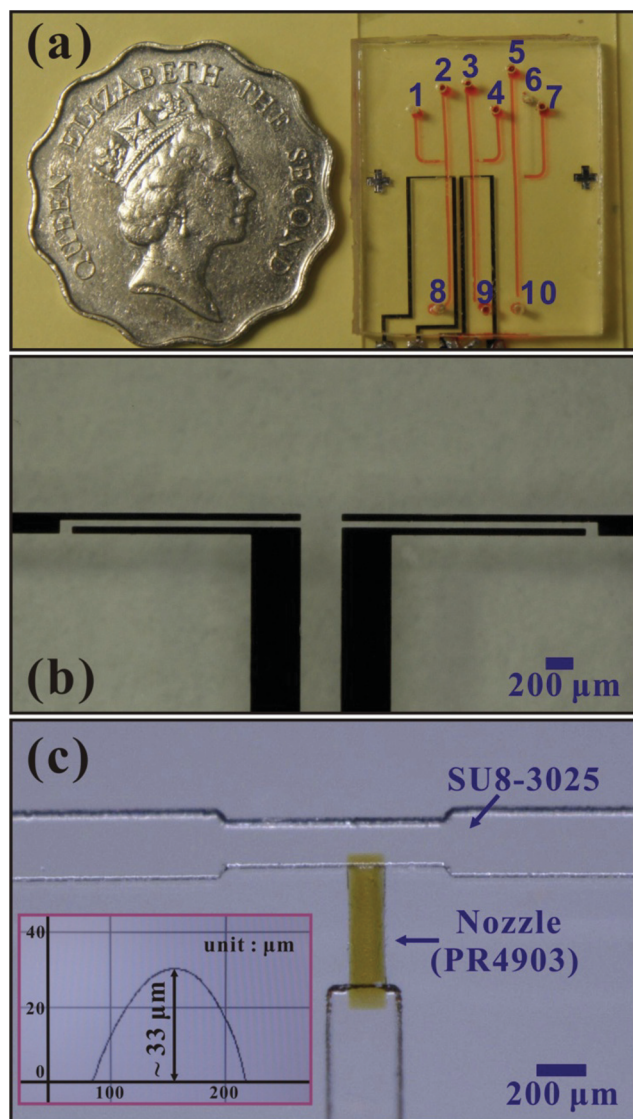


Fig. 5 (a) Optical image of the microfluidic chip, all flow channels are filled with colored oil for contrast; (b) enlarged image of the embedded detecting electrodes; (c) illustration of the flow channel layer master. The inset shows the cross-sectional profile of the connecting nozzle.

gap. Fig. 5(c) is the optical image taken from the flow channel layer master. PR4903 was used to connect the two branches (made from SU8-3025) forming the T-junction. One of the branches is the carrier fluid inlet while the other is the signal inlet. The inset of Fig. 5(c) shows the cross-sectional profile of the nozzle measured by the Surface Profiler (KLA-TENCOR P-10 Profiler). The measurement has confirmed that the shape of the nozzle is round. The rounded shape of the nozzle is significant for ensuring complete sealing. The input air pressure used in our experiment was 200 kPa when the valve was fully closed.

Universal logic gate demonstration

In our experiment, saturated Na_2SO_4 solution was used as conductive droplets at the signal inlet and colored sunflower oil was adopted as the insulating carrier fluid. The conductive

microdroplet can be regarded as a resistive component in the droplet detection circuit. For simplicity, R_D is used to represent the equivalent resistance for a conductive droplet. While for the carrier fluid, we assume its resistance is enormously large when compared to the conductive droplet ($R_{\text{oil}} \sim \infty \Omega$). As explained in the second section, for the input fluidic signals, state “1” indicates that a conductive droplet (Na_2SO_4) is present at the detecting electrode pair and state “0” indicates that insulating carrier fluid is passing through the electrode. For the output fluidic signal, state “0” indicates that the membrane is deflected and no droplet is injected to the output port while state “1” indicates the contrary. From such a perspective, fluid inputs A and B can have four different combinations of values: (0, 0), (0, 1), (1, 0) and (1, 1). Table 1 lists the truth values of the outputs for different logic functions, based on different input signals (A, B).

Various logic functions can be achieved by changing the voltages of V_{12} and V_{34} . The voltages can be adjusted by a resistive circuit on the external circuit board, with a voltage variation of ± 9.0 V. Experimental data on the voltages applied for each logic function are summarized in Table 2. In the successful demonstration of the universal logic gate operation, the threshold voltage of the triggering circuit was set within the range of 1.8–2.0 V. Values of V_{12} and V_{34} were carefully set to achieve the corresponding logic functions as shown in Table 2. In fact, one can achieve any logic function by selecting a series of voltage combinations for V_{12} and V_{34} , and the associated threshold voltage. Table 2 illustrates one possible solution to the truth table. The experimental results for the common logic functions such as AND, IF and OR are shown in Fig. 6(a)–(c). For the AND function, the output is true only when microdroplets are presented simultaneously at the detecting locations A and B. For the IF-A function, the output is true when the input signal A is true regardless of the value of the input signal B. The result for the IF-B function is similar. As for the OR function, the output is false only when the input signals A and B are both absent. (For the experimental results of other logic functions, please see the ESI†).

In the following, we select the NAND function as an example to explain how the logic operation can be realized using the liquid-electronic hybrid divider. Fig. 7(a)–(d) show the behavior of output fluidic signals based on different input signals (A, B). The respective logic values for A and B at the inputs are marked in Fig. 7(a)–(d). For the NAND function, the output is false (state “0”) only when the two inputs (A and B) are both true (state “1”). The corresponding equivalent circuits for Fig. 7(a)–(d) are illustrated in Fig. 7(e). The voltages at nodes 2 and 3 are set to be +3.0 V and –3.0 V respectively, while nodes 1 and 4 are connected to the ground. Using R_D to define the equivalent resistance, the voltages at A and B can be written as:

$$V_A = \frac{RV_2 + R_D V_1}{R + R_D} \quad (1)$$

$$V_B = \frac{RV_3 + R_D V_4}{R + R_D} \quad (2)$$

where resistance $R = R_A = R_B \approx 10 \text{ M}\Omega$.

When a conductive droplet flows through node A (B), V_A (V_B) drops to about +1.3 V (–1.3 V). Under these circumstances,

Table 1 Truth table of universal logic gates with two inputs (A, B)^a

Input (A, B)	Logic function/output (OP)											
	FALSE	AND	A B	IFA	XOR	OR	NOR	XNOR	NOTA	A → B	NAND	TRUE
(0, 0)	0	0	0	0	0	0	1	1	1	1	1	1
(0, 1)	0	0	0	0	1	1	0	0	1	1	1	1
(1, 0)	0	0	1	1	1	1	0	0	0	0	1	1
(1, 1)	0	1	0	1	0	1	0	1	0	1	0	1

^a For B A, B → A, IF B and NOT B, functions are similar to A B, A → B, IF A, and NOT A, respectively.

there are four values of ΔV generated: 0 V, 1.3 V, 1.3 V and 2.6 V, as illustrated by Fig. 7(a), (b), (c) and (d) respectively. Only for the last case as shown in Fig. 7(d) where both conductive droplets are presented simultaneously at inputs A and B (representing input logic values of (1, 1)), the measured ΔV (= 2.6 V) is larger than the built-in threshold voltage ($V_g = 2.0$ V). The result is the activation of the PAV which sets the output to an OFF state (representing an output logic value of “0”) where no fluidic droplet is released.

Droplet-based chemical reaction demonstration—an application of the hybrid divider

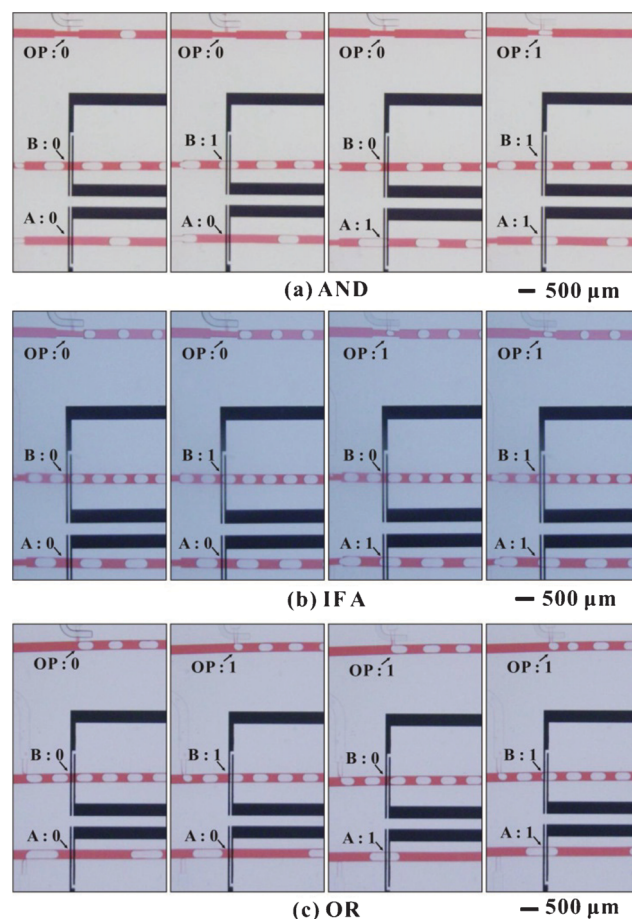
We have successfully demonstrated a self-induced, on-demand droplet-based chemical reaction using the IF function modified from the universal logic gate structure mentioned previously. Fig. 8(a) shows the design of the microfluidic chip employed for such a chemical reaction. A similar fabrication process employed by the universal logic gate was used to realize the microfluidic chip design, but with only two flow channels. Inlets 1 and 5 are for reagent injection while inlets 3 and 4 are for the carrier fluid. The detecting electrodes are embedded in the microchannel on the right so that the PAV is placed on top of the nozzle on the left channel. In this configuration, inlet A acts as the input signal while inlet B is the output. An array of micropillars made of PDMS are embedded inside the microchannel which decreases the flow rate of the reagents, allowing effective merging, mixing and chemical reaction. A photo of the fabricated chip is shown in Fig. 8(b). Fig. 8(c), (d) and (e) illustrate the experimental results for the droplet-based chemical reaction based on the IF function.

Table 2 Combinations of applied voltages used in the universal logic gate with two input variables^{a,b}

Logic function	Voltage supply (V)					
	Node 1	Node 2	$ V_{12} $	Node 3	Node 4	$ V_{34} $
FALSE	+5.0	GND	5.0	GND	GND	0
TRUE	GND	GND	0	GND	GND	0
IF(A)	+3.0	GND	3.0	GND	GND	0
NOT(A)	GND	+5.0	5.0	GND	GND	0
AND	+2.0	GND	2.0	GND	-2.0	2.0
OR	+3.0	GND	3.0	+3.0	GND	3.0
NAND	GND	+3.0	3.0	-3.0	GND	3.0
NOR	GND	+5.0	5.0	-5.0	GND	5.0
XOR	GND	+6.0	6.0	GND	+2.0	2.0
XNOR	GND	+5.0	5.0	+5.0	GND	5.0
A B	+3.0	GND	3.0	-3.0	GND	3.0
A → B	GND	+5.0	5.0	+3.0	GND	3.0

^a For B A, B → A, IF B and NOT B, voltage arrangements are similar to A B, A → B, IF A, and NOT A. ^b The threshold voltage of the triggering circuit is set to be in range of 1.8 V to 2.0 V.

When no conductive droplet (of NaSCN solution) appears at the parallel electrodes, the output signal is “0”, represented by no droplet (of FeCl₂ solution) at B. Only when a conductive droplet passes over the detecting electrodes (Fig. 8(d)), is the output fluidic signal activated and emerges as a colourless droplet at output B. When two colourless droplets arrive at the array of micropillars, mixing and reaction occur resulting in a colour change as shown in Fig. 8(e). The experimental results reveal that the chemical reaction based on droplet microfluidics can be well controlled and conducted with the help of logic functions realized by the design of the liquid-electronic hybrid divider. With the aid of these logic functions, a micro-reactor can be readily achieved with digitized microfluidic signals. The impact of a micro-reactor can be potentially useful for customized on-chip manipulation of droplet-based chemical action for biological or chemical analysis.

**Fig. 6** Experimental results of logic functions: AND, IF-A and OR.

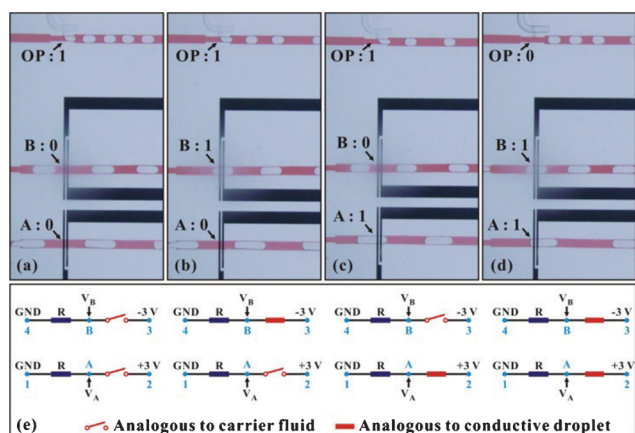


Fig. 7 (a)–(d) Optical images of the experimental results for the NAND logic function; (e) corresponding equivalent circuits for different input signals (A, B) as depicted in (a)–(d).

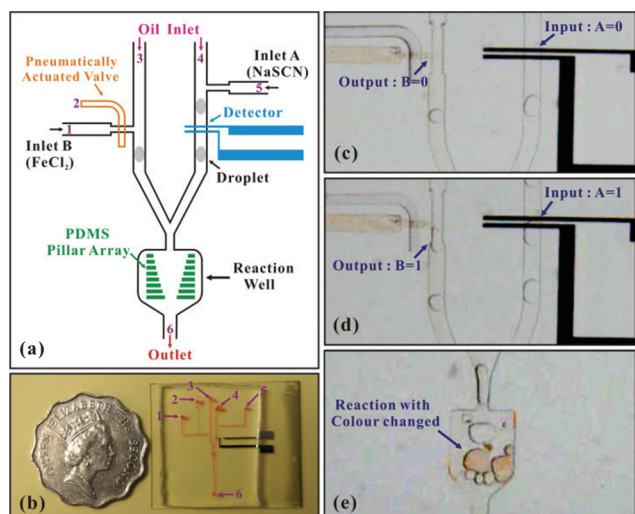


Fig. 8 (a) Design of the microfluidic chip for droplet-based chemical reaction; (b) optical image of the fabricated microfluidic chip; (c)–(e) optical images showing the real-time chemical reaction achieved by the IF logic function.

Conclusions

We have successfully proposed, fabricated, and tested the performance of a hybrid platform for universal logic gate operation. All 16 logic computations with two fluidic inputs have been implemented by defining the threshold voltages. The performance of the on-chip PAV has been proved to be capable of accurate and on-demand control of the generation of output fluidic signal. The dual-layer architecture, which can be constructed by standard photolithography and soft-lithography techniques, allows chip integration and the realization of large-scale and complex logic computations. Programmable and self-induced microdroplet-based chemical reaction based on the IF function has also been achieved using a similar technique. The

universal logic gate based on digitized microfluidics can be employed for accurate micro-volume chemical reaction for self-contained and on-demand biological and chemical analysis, as well as on-chip fluidic computation and control.

Acknowledgements

This publication is based on work partially supported by Award No. SA-C0040/UK-C0016, made by King Abdullah University of Science and Technology (KAUST), and Hong Kong RGC grants HKUST 604710 and 605411.

References

- 1 H. Song, D. L. Chen and R. F. Ismagilov, *Angew. Chem., Int. Ed.*, 2006, **45**, 7336–7356.
- 2 M. Y. Zhang, X. Q. Gong and W. J. Wen, *Electrophoresis*, 2009, **30**, 3116–3123.
- 3 A. Huebner, S. Sharma, M. S. Art, F. Hollfelder, J. B. Edel and A. J. deMello, *Lab Chip*, 2008, **8**, 1244–1254.
- 4 Z. T. Cygan, J. T. Cabral, K. L. Beers and E. J. Amis, *Langmuir*, 2005, **21**, 3629–3634.
- 5 F. Jousse, G. Lian, R. Janes and J. Melrose, *Lab Chip*, 2005, **5**, 646–656.
- 6 X. Niu, S. Gulati, J. B. Edel and A. J. deMello, *Lab Chip*, 2008, **8**, 1837–1841.
- 7 P. Singh and N. Aubry, *Electrophoresis*, 2007, **28**, 644–657.
- 8 D. R. Link, S. L. Anna, D. A. Weitz and H. A. Stone, *Phys. Rev. Lett.*, 2004, **92**, 054503.
- 9 N. R. Beer, E. K. Wheeler, L. L. Houghton, N. Watkins, S. Nasarabadi, N. Hebert, P. Leung, D. W. Arnold, C. G. Bailey and B. W. Colston, *Anal. Chem.*, 2008, **80**, 1854–1858.
- 10 P. Watts and S. J. Haswell, *Chem. Eng. Technol.*, 2005, **28**, 290–301.
- 11 H. Song, J. D. Tice and R. F. Ismagilov, *Angew. Chem., Int. Ed.*, 2003, **42**, 768–772.
- 12 B. Zheng, C. J. Gerdt and R. F. Ismagilov, *Curr. Opin. Struct. Biol.*, 2005, **15**, 548–555.
- 13 E. Um, D. S. Lee, H. B. Pyo and J. K. Park, *Microfluid. Nanofluid.*, 2008, **5**, 541–549.
- 14 D. W. M. Marr and T. Munakata, *Commun. ACM*, 2007, **50**, 64–68.
- 15 T. Munakata and D. W. M. Marr, *IASTED Biomedical Engineering*, 2005, **2005**, 519–523.
- 16 W. Zhan and R. M. Crooks, *J. Am. Chem. Soc.*, 2003, **125**, 9934–9935.
- 17 A. Groisman, M. Enzelberger and S. R. Quake, *Science*, 2003, **300**, 955–958.
- 18 T. Vestad, D. W. M. Marr and T. Munakata, *Appl. Phys. Lett.*, 2004, **84**, 5074–5075.
- 19 S. Kou, H. N. Lee, D. van Noort, K. M. K. Swamy, S. H. Kim, J. H. Soh, K. M. Lee, S. W. Nam, J. Yoon and S. Park, *Angew. Chem., Int. Ed.*, 2008, **47**, 872–876.
- 20 M. Prakash and N. Gershenfeld, *Science*, 2007, **315**, 832–835.
- 21 L. F. Cheow, L. Yobas and D. L. Kwong, *Appl. Phys. Lett.*, 2007, **90**, 054107.
- 22 M. W. Toepke, V. V. Abhyankar and D. J. Beebe, *Lab Chip*, 2007, **7**, 1449–1453.
- 23 Y. Zhao and K. Chakrabarty, *IEEE Trans. Biomed. Circuits Syst.*, 2010, **4**, 250–262.
- 24 M. Y. Zhang, L. M. Wang, X. Wang, J. Wu, J. X. Li, X. Q. Gong, J. H. Qin, W. H. Li and W. J. Wen, *Soft Matter*, 2011, **7**, 7493–7497.
- 25 M. A. Unger, H. P. Chou, T. Thorsen, A. Scherer and S. R. Quake, *Science*, 2000, **288**, 113–116.
- 26 A. M. Leshansky and L. M. Pismen, *Phys. Fluids*, 2009, **21**, 023303.
- 27 J. H. Xu, S. W. Li, J. Tan and G. S. Luo, *Microfluid. Nanofluid.*, 2008, **5**, 711–717.